Journal of Anatomy

J. Anat. (2010) **216**, pp407–416 doi: 10.1111/j.1469-7580.2009.01190.x

Distribution and expression of CD200 in the rat respiratory system under normal and endotoxin-induced pathological conditions

Ya-Fen Jiang-Shieh,[1] Hsiung-Fei Chien,[2] Chiu-Yun Chang,[3] Tsui-Shan Wei,[1] Mei-Miao Chiu,[4] Hui-Min Chen[3,5] and Ching-Hsiang Wu[3,6]

[1]*Department of Anatomy, College of Medicine, National Cheng Kung University, Tainan, Taiwan*
[2]*Department of Surgery, College of Medicine, National Taiwan University, Taipei, Taiwan*
[3]*Department of Anatomy, College of Medicine, Taipei Medical University, Taipei, Taiwan*
[4]*Institute of Anatomy and Cell Biology, School of Medicine, National Yang-Ming University, Taipei, Taiwan*
[5]*Electron Microscopy Center, College of Medicine, Taipei Medical University, Taipei, Taiwan*
[6]*Department and Institute of Biology and Anatomy, National Defense Medical Center, Taipei, Taiwan*

Abstract

In vivo and *in vitro* studies have clearly demonstrated that signaling mediated by the interaction of CD200 and its cognate receptor, CD200R, results in an attenuation of inflammatory or autoimmune responses through multiple mechanisms. The present results have shown a differential expression of CD200 in the respiratory tract of intact rats. Along the respiratory passage, CD200 was specifically distributed at the bronchiolar epithelia with intense CD200 immunoreactivity localized at the apical surface of some ciliated epithelial cells; only a limited expression was detected on the Clara cells extending into the alveolar duct. In the alveolar septum, double immunofluorescence showed intense CD200 immunolabeling on the capillary endothelia. A moderate CD200 labeling was observed on the alveolar type II epithelial cells. It was, however, absent in the alveolar type I epithelial cells and the alveolar macrophages. Immunoelectron microscopic study has revealed a specific distribution of CD200 on the luminal front of the thin portion of alveolar endothelia. During endotoxemia, the injured lungs showed a dose- and time-dependent decline of CD200 expression accompanied by a vigorous infiltration of immune cells, some of them expressing ionized calcium binding adapter protein 1 or CD200. Ultrastructural examination further showed that the marked reduction of CD200 expression was mainly attributable to the loss of alveolar endothelial CD200. It is therefore suggested that CD200 expressed by different lung cells may play diverse roles in immune homeostasis of normal lung, in particular, the molecules on alveolar endothelia that may control regular recruitment of immune cells via CD200-CD200R interaction. Additionally, it may contribute to intense infiltration of immune cells following the loss or inefficiency of CD200 under pathological conditions.

Key words endotoxin; immunoglobulin superfamily; lung epithelia; pulmonary endothelia.

Introduction

CD200 is a transmembrane glycoprotein containing two extracellular immunoglobulin domains and lacks intracellular signaling motifs or docking sites for adapter signaling molecules (Barclay et al., 1986). CD200 is the ligand for a receptor CD200R, whose expression is restricted to hemopoietic cells, particularly myeloid cells (Wright et al., 2000). *In vivo* and *in vitro* studies have demonstrated unequivocally that signaling mediated by CD200–CD200R interaction results in an attenuation of inflammatory or autoimmune responses through multiple mechanisms (Hoek et al., 2000; Wright et al., 2000). By contrast, however, there is an apparent lack of information on CD200 expression under normal and/or pathological conditions. CD200 expression has been found to be related to normal development and aging (Bartolome et al., 2002; Frank et al., 2006). In the center of chronic active and inactive multiple sclerosis lesions, CD200 was down-regulated (Koning et al., 2007). In

Correspondence
Dr. Ching-Hsiang Wu, Department and Institute of Biology and Anatomy, National Defense Medical Center, 161, Sec. 6, Min-Chuan East Road, Taipei 114, Taiwan. T: + 88 6 2 87910787; F: + 886 2 87910787; E: microgli@mail.ndmctsgh.edu.tw
and
Dr. *Hsiung-Fei Chien, MD PhD, Department of Surgery, College of Medicine, National Taiwan University, No. 1, Section 1, Jen-Ai Road, Taipei, 100, Taiwan. T: +886 2 23123456 ext 65594; F: +886 2 23568810; E: hfchien@ntu.edu.tw*

Accepted for publication *20 November 2009*
Article published online *7 January 2010*

metastatic melanoma, CD200 may also be induced by extracellularly regulated protein kinase pathways to tone down a host of antitumor immune responses (Petermann et al., 2007). It is widespread in a variety of tissues, including the nervous system, activated T-cells, B-cells, dendritic cells in lymphatic follicles, cells of glomeruli and ovarian degenerating follicles and vascular endothelium (Clark et al., 1985; Barclay et al., 1986; McCaughan et al., 1987). CD200 is also distributed at the epithelium-derived tissues such as the thymus, retinas and hair follicles (Ragheb et al., 1999; Dick et al., 2001; Rosenblum et al., 2004). The existence of CD200 in other epithelia covering the gastrointestinal, urogenital and respiratory tracts has not yet been fully explored. In the respiratory tract, adhesion molecules belonging to the immunoglobulin superfamily such as intracellular adhesion molecule (ICAM), neural cell adhesion molecule, neural cell adhesion molecule L1, melanoma cell adhesion molecule, receptor for advanced glycation end-products (RAGE) and tumor suppressor in lung cancer 1 have been well documented (Jaques et al., 1993; Chalepakis et al., 1994; Feuerhake et al., 1998; Schulz et al., 2003; Bartling et al., 2005). Clinical and experimental surveys have also revealed a close relationship between these adhesion molecules and the pathogenesis of multiple respiratory disorders. Beck-Schimmer et al. (2002) have reported that ICAM was constitutively expressed at low levels by alveolar epithelial cells and rapidly up-regulated during inflammation and pulmonary fibrosis by mediating the accumulation of leukocytes. Moreover, an involvement of ICAM-1 in small-cell lung carcinoma and down-regulation of RAGE were considered a critical step in tissue reorganization and the formation of lung tumors (Finzel et al., 2004; Bartling et al., 2005). As an adhesion molecule and being a member of the immunoglobulin superfamily, it was surmised that CD200 might exist in the rat airway. On the other hand, how CD200 is modulated, if it were to exist in the lung tissues, especially during inflammation, is not known. The present study is therefore aimed to investigate the distribution of CD200 in intact rat lungs and to characterize the cellular elements that may express CD200 expression in the pulmonary tissues. The possible changes of CD200 expression in the pulmonary tissues in systemic sepsis are also analyzed.

Materials and methods

Animal procedure and tissue processing

Male Wistar rats (n = 55), weighing 250–300 g, were used. They were anesthetized with 7% chloral hydrate (0.4 mL per 100 g body weight, C8383; Sigma) and 15 of these rats received an intratracheal injection of 1 mg kg^{-1} lipopolysaccharide (LPS, from *Escherichia coli*, serotype 055:B5, L-2880; Sigma). The control rats (n = 5) received the same volume of saline intratracheally. The treated rats were sacrificed 24 h after injection. For immunohistochemistry, all animals were fixed by intracardiac perfusion with 50 mL normal saline followed by 200 mL of 4% paraformaldehyde in 0.1 M phosphate buffer (PB), pH 7.4. The trachea and lung were removed and immersed in the same fixative for 2 h and kept in 0.1 M PB containing 30% sucrose overnight at 4 °C. For Western blotting, the rats were given an intratracheal injection of LPS at dosages 0.1, 1 or 2.5 mg kg^{-1} (n = 5, for the respective dosage); rats (n = 5) receiving an equal volume of saline served as the matching controls. After 24 h, animals were anesthetized with 7% chloral hydrate (10 mg kg^{-1}) and the lung tissues were removed and kept at −80 °C until use. Other rats that were intratracheally injected with 1 mg kg^{-1} LPS were allowed to survive for 12, 24 and 48 h (n = 5 at each time point) before sacrifice. All animals had free access to food and water at all times. For animal care and surgical procedures, we followed the Guide for the care and use of laboratory animals published by National Institutes of Health. The University Laboratory Animal Care and Use Committee of the National Defense Medical Center approved all surgical protocols.

Immunohistochemistry

Immunoperoxidase labeling

The trachea and lung tissues were cut at 10-μm thickness in a cryostat. The sections were pretreated with 1% H_2O_2 for 1 h to block any possible endogenous peroxidase and then with 10% normal horse serum for 1 h. The sections were incubated in monoclonal anti-CD200 antibody (1 : 100, MCA44G; Serotec) that was diluted with 0.05 M Tris-buffer saline (TBS, pH 7.4) containing 0.1% Triton X-100 overnight. Subsequent antibody detection was carried out using the biotinylated horse anti-mouse IgG (1 : 300, BA-2001; Vector). The immunoreaction was visualized using 0.025% 3,3′-diaminobenzidine tetrahydrochloride (DAB, D5637; Sigma). Control sections were incubated in the absence of primary antibody. The sections were then counterstained with methyl green and examined under a light microscope equipped with a digital camera.

Double immunofluorescence labeling

The sections were pretreated with 10% normal horse serum for 1 h. They were incubated with monoclonal anti-CD200 antibody and one of the following primary antibodies: rabbit anti-podoplanin (for alveolar type I cell, 1 : 2000, P1995; Sigma), rabbit anti-prosurfactant-C [for alveolar type II cell (ATII), 1 : 2000, AB3786, Chemicon], rabbit anti-Clara cell secreting protein (CCSP for Clara cell, 1 : 2000, 07-623, Upstate) or rabbit anti-ionized calcium binding adapter protein 1 [IBA1, identical to allograft inflammatory factor-1 (AIF-1), for macrophage and immune cells, 1 : 2000, 019-1974, Wako]. The sections were incubated in primary antibodies with 0.05 M TBS (pH 7.4) containing 0.1% Triton X-100 overnight at 4 °C. Subsequent antibody detection was carried out using goat anti-rabbit IgG-conjugated fluorescein isothiocyanate (1 : 300, 111-096-003; Jackson ImmunoResearch) or goat anti-mouse IgG-conjugated cyanine dye 3 (1 : 300, 115-165-100; Jackson ImmunoResearch) for 2 h. The sections were visualized by propidium iodide nuclear counterstaining and then examined in a confocal laser scanning microscope (LSM510; Zeiss).

Electron microscopy

The lungs were trimmed into 1–2-mm-thick blocks. Specimens were incubated with mouse anti-rat CD200 antibody for immuno-electron microscopy as in light microscopy but with the

substitution of 0.01% Triton X-100 used in the solutions. All sections were then rinsed in PB, post-fixed with 1% O_5O_4 dissolved in 0.1 M PB, dehydrated with alcohol and embedded in Epon-Araldite mixture. Ultrathin sections were obtained using a diamond knife. Tissue sections without routine double staining were examined and photographed under a Hitachi 600 electron microscope with a CCD camera attached.

Western blotting analysis

The lungs were homogenized in a lysine buffer containing 10% protease inhibitor cocktail (S8820; Sigma) and then sonicated. The homogenate was centrifuged and the supernatant was collected. Following quantification of total protein (Bio-Rad protein assay), the tissue samples were diluted 1/4 with SDS sample buffer and boiled at 100 °C for 5 min. Prestained protein ladders (SM0671; Fermentas) were used to determine the molecular weight of the immunoreactive bands. Protein samples (100 μg protein per gel lane) were loaded on a 12% acrylamide-SDS gel, and electrotransferred to PVDF membrane (162-0177; Bio-Rad). Non-specific sites were blocked by incubating the membrane with TBS containing 10% dry milk and 0.1% Tween 20 for 12 h and then incubated with anti-CD200 antibody (1 : 200, MCA44G; Serotec) at 4 °C overnight. After washing with TBST (TBS containing 0.1% Tween 20), membranes were incubated with horseradish peroxidase-conjugated secondary anti-mouse antibody (1 : 5000, 115-035-146; Jackson ImmunoResearch) for 2 h. Specific binding was revealed by chemiluminescent HRP substrate (WBKLS0500; Millipore). For loading control, the membranes were reprobed with a monoclonal anti-β-actin (1 : 1000, A5441; Sigma). The Western blots used for statistical analysis were performed in triplicate. The quantitative data are presented as mean ± SE. Statistical comparison was done using ANOVA followed by *post hoc* Tukey's multiple comparison tests. Differences were considered significant at $P < 0.05$.

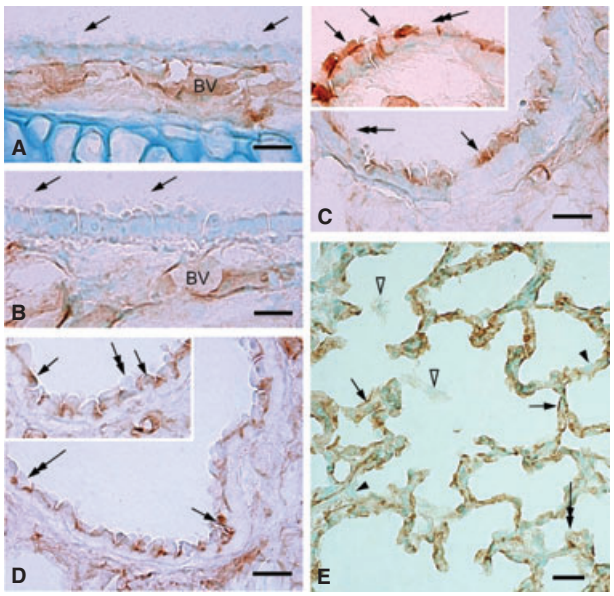

Fig. 1 (A–E) CD200 immunoreactivity in the conducting airways of intact rat lungs. CD200 labeling is localized consistently at the blood vessels (A–B, BV) along the airways but is absent at the epithelia of the nasal cavity, trachea (A, arrows) and bronchus (B, arrows). CD200 immunoreactivity of varying intensity appears initially at the bronchioles, particularly at specific groups of the ciliated epithelial cells (C, inset, arrows) and Clara cells (D, inset, arrows); some cells are CD200-negative (C–D, inset, double-headed arrows). In the alveolar tissues, CD200 staining along the alveolar septum appears discontinuous (E, arrows). Other cells/structures are not clearly defined as CD200-positive except for some type II pneumocytes which show a unique vacuolated cytoplasm containing weak but detectable CD200 immunoreactive product (E, double-headed arrow). Other epithelial cells (E, arrowheads) and alveolar macrophages (E, open arrowheads) are clearly negative for CD200. Scale bars: 20 μm.

Results

In the respiratory duct, CD200 immunoreactivity was absent at the epithelia of the trachea and bronchus (Fig. 1A,B). It was, however, observed consistently in the underlying blood vessels. CD200 labeling appeared to be associated with some epithelial cells of the bronchioles, especially at the apical cilia (Fig. 1C). The CD200-positive epithelial cells were concentrated at the respiratory bronchiole. Intercalated between the labeled epithelial cells were some Clara cells which exhibited CD200 immunoreactivity (Fig. 1D). CD200 immunoreactivity in Clara cells was relatively weak when compared with the labeled ciliated epithelia. In the alveolar tissue, a diffuse or discontinuous labeling pattern of CD200 was observed along the alveolar septum (Fig. 1E); most labeling appeared to be localized at the alveolar capillaries. Some alveolar type II epithelial cells characterized by the vacuolated cytoplasm were also weakly labeled with CD200 (Fig. 1E). Alveolar macrophages were devoid of CD200 immunoreactivity (Fig. 1E).

To confirm the distribution of CD200 in the lung structures, double immunofluorescence staining of CD200 combined with specific antibodies against pulmonary cell elements was carried out. Confocal microscopic observation showed the colocalization of CD200 with pro-surfactant-C (Fig. 2C) or Clara cell secretory protein (Fig. 2D), a specific marker for type II pneumocyte or Clara cell, respectively. Type II pneumocytes marked by pro-surfactant-C antibody exhibited CD200 only along their apical surface (Fig. 2C). The remaining epithelia such as type I pneumocytes marked specifically by podoplanin antibody showed a continuous lineal labeling outline along the septum (Fig. 2A). Podoplanin immunoreactivity, however, was rarely colocalized with CD200 (Fig. 2A). On closer examination, it was found that site of CD200 immunoreactivity was close to but clearly beneath the podoplanin labeling (Fig. 2B), indicating that type I pneumocytes may be negative for CD200 (see below). The underlying alveolar endothelia were intensely labeled for CD200.

Immunoelectron microscopy confirmed intense CD200 expression on alveolar endothelial cells but its apparent absence in type I pneumocytes. A feature worthy of note was the localization of endothelial CD200 immunoreaction product on the luminal front of the thin portion of

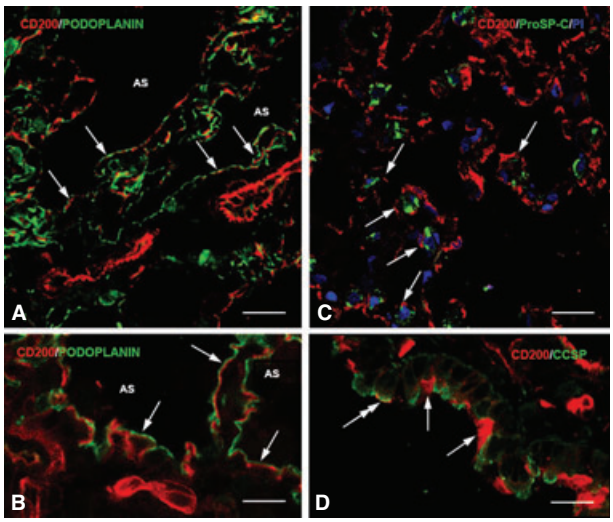

Fig. 2 (A–D) Immunofluorescence micrographs showing double labeling of CD200 (red) with podoplanin (alveolar type I cell marker, A–B, green), pro-surfactant-C (alveolar type II cell marker, C, green) or Clara cell secretory protein (Clara cell maker, D, green). Note that most CD200 immunoreactivity does not overlap with podoplanin, which appears to lie parallel to or above CD200 (A–B, arrows) and faces the airspace (AS). After staining with the nuclear dye propidium iodide (PI), alveolar type II cells show granule-like immunoreactivity of pro-surfactant-C and are incompletely outlined by weak CD200 immunoreactivity (C, arrows). In D, most Clara cells exhibit very weak CD200 labeling amongst the intensely-labeled cilia (arrows). Only a Clara cell shows significant CD200 on its apical membrane (D, double-headed arrow). Scale bars: (A,C–D) 20 μm, (B) 10 μm.

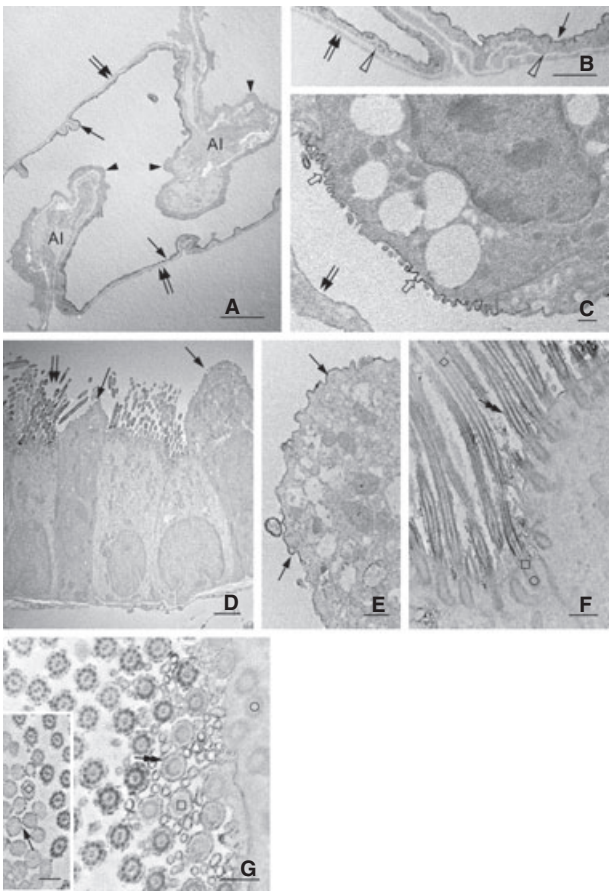

Fig. 3 (A–G) Electron micrographs showing CD200 immunoreactivity in intact rat lungs. A preferential distribution of CD200 is observed at the luminal cytoplasmic membrane (A,B, arrows) of alveolar endothelia forming blood–air barrier. CD200 is negligible or absent on the remaining front of endothelia (A, arrowheads) or on the area that is facing the alveolar interstitium (A, AI). Moreover, the abluminal wall of alveolar endothelia (B, open arrowheads) and the alveolar type I epithelia (A–C, double arrows) were totally negative for CD200. Alveolar type II epithelial cells show CD200 expression exclusively on their apical cytoplasmic membrane furnished with short microvilli (C,). In the conducting airways, CD200 reaction product is distributed at the apical membrane of Clara cells (D–E, arrows) and cilia (D, double arrows) on the bronchiolar epithelia. Some cilia show a progressively increased CD200 immunoreactivity along the microtubule bundle in an apical to basal gradient (F). Microtubule bundles or axonemes constituting the most apical part (F, inset, ◇), base (F–G, □) and connecting basal body (F–G, ○) of the cilium show lack of CD200. The ciliary membrane also exhibits CD200 that is confined to the most apical (inset in G, arrow) and basal (F–G, double-headed arrows) parts; it is, however, inconsistent at the middle region of the cilium. Scale bars: (D) 2 μm; (E–G), inset in (G) 0.5 μm.

endothelia; it was, however, weakly expressed or absent on the thick portion of the cells (Fig. 3A,B). The abluminal wall of alveolar endothelia showed a lack of CD200 immunoreaction product (Fig. 3A,B). Type II pneumocytes displayed CD200 reaction product which was confined to their apical plasma membrane and microvilli facing the airspace (Fig. 3C). The remaining structures of the cell were CD200-negative. A similar labeling pattern was also found on Clara cells (Fig. 3D,E). In the labeled ciliated epithelia, CD200 immunoreaction product delineated the most apical and basal parts of the ciliary membrane. In the middle region, CD200 immunoreaction product was inconsistent (Fig. 3F,G). Ultrastructural studies further revealed that CD200-positive cilia showed an increasing CD200 immunoreactivity along the microtubule bundles (axoneme) in an apical–basal gradient (Fig. 3F,G). The most apical and base parts of the microtubule bundles and connecting basal body of the cilium were devoid of CD200 immunoreaction products (Fig. 3F,G).

Cell adhesion molecules (CAMs) of the immunoglobulin superfamily are well known to be regulated by endotoxin (Beck-Schimmer et al., 2002). Belonging to the same family, CD200 has been implicated in immunosuppression in immune diseases (Hoek et al., 2000; Wright et al., 2000). To test the possible modification of lung CD200 expression, LPS at different concentrations was administered by intratracheal instillation to examine the changes of pulmonary CD200 in acute lung injury of rats at various time points. During endotoxemia, Western blot analysis showed a significant decline in CD200 expression in the injury lungs challenged with 1 or 2.5 mg kg^{-1} of LPS for 24 h (Fig. 4A). The dramatic decrease in lung CD200 expression was induced as early as 12 h after LPS (1 mg kg^{-1}) instillation; expression was gradually restored at 24 and 48 h (Fig. 4B).

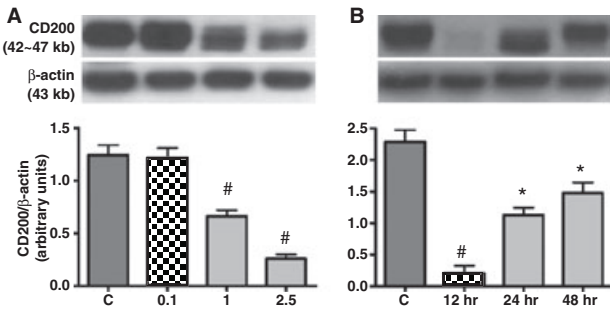

Fig. 4 (A–B) Western blot analysis of CD200 expression in rat lung. Adult rats are intratracheally instilled with an increasing concentration (0.1, 1 or 2.5 mg kg^{-1}) of LPS for 24 h (A), or others with 1 mg kg^{-1} LPS for different time intervals (12, 24 or 48 h) (B). Representative Western blots are shown in upper frames and relative levels of CD200 expression determined by densitometric scanning of the CD200 bands and normalized to the β-actin signal are shown in the bar graphs. Data shown are the mean ± SE of at least three separate experiments and are presented as the CD200/β-actin ratio. Statistical significance is established by ANOVA followed by *post hoc* Tukey's multiple comparison tests. #$P < 0.01$ vs. each group; *$P < 0.01$ vs. the control or 12 h-treatment of LPS. In rats treated with different doses of LPS (A), lung CD200 is significantly reduced after treatment with 1–2.5 mg kg^{-1} LPS, whereas 0.1 mg kg^{-1} does not change the expression. The significant reduction of lung CD200 is evident as early as 12 h post-challenge with 1 mg kg^{-1} LPS (B). The CD200 reduction continues and expression is restored at 24 and 48 h post-challenge, but the expression levels at these time intervals are not statistically different (B).

Immunoperoxidase staining confirmed a decreased expression of CD200 in lungs challenged with LPS, although the latter induced different degrees of injury at different regions of the same lung (Fig. 5A–D). Irrespective of tissue injury levels, CD200 immunoreactivity in Clara cells and ciliated epithelia in the bronchioles remained unaltered (data not shown). In the mild injured tissues, CD200 staining was pale and more diffuse in the alveolar septum; it was equally weak in type II pneumocytes when compared to the saline-treated lung (Fig. 5A–D). More small round cells exhibiting dense nucleus appeared in the septum and expressed CD200 (Fig. 5B). In severe injury tissues with low expression of CD200, CD200 immunoreactivity in type II pneumocytes appeared to be accentuated in the light background (Fig. 5E). The alveolar septum became thickened and was invaded by more immune cells, including CD200-positive lymphocyte-like cells (Fig. 5E). The infiltrated immune cells were further examined by double immunofluorescence staining with antibody against IBA1/AIF-1 that is expressed in the endothelium of pulmonary vessels and in inflammatory cells, including T cells and macrophages in the lung of patients with systemic sclerosis (Del Galdo et al., 2006). Consistent with the immunoperoxidase staining of CD200, the present results showed a reduced CD200 immunofluorescence in the LPS-challenged alveolar tissues (Fig. 6A,D) and more IBA1/AIF-1 labeled inflammatory cells infiltrating into the perivascular zone of the pulmonary vessels and into the

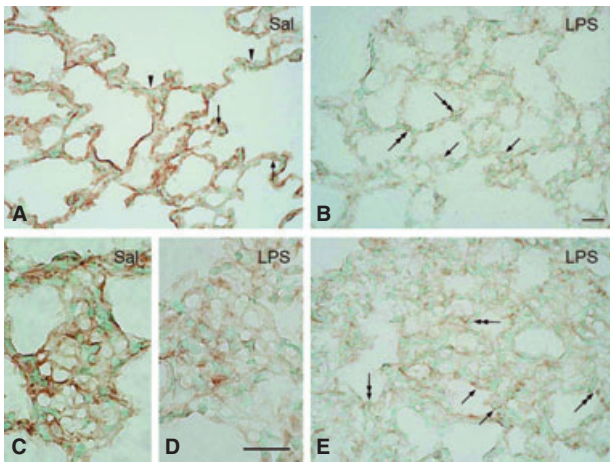

Fig. 5 (A–E) CD200 expression in the alveolar sac of rats intratracheally instilled with saline (Sal) or LPS for 24 h. In the Sal-treated (A) lung, CD200 immunoreactive product is clear but discontinuous along the alveolar septum (A, arrowheads). Weak immunoreactivity is found on alveolar type II epithelial cells with vacuolated cytoplasm (A, arrows). After LPS challenge (B), CD200 immunoreaction product is markedly reduced and appears attenuated along the septum where ATII shows a similar and weak immunoreactivity (B, arrows). Numerous lymphocyte-like cells (B, double-headed arrows) with a dense nucleus are clearly positive for CD200 and occupy the septum. In a tangential section of the septum, an obvious capillary network with intense immunoreactivity is observed in the Sal-treated lung (C); this becomes inconspicuous after LPS instillation (D). In areas with severe injury, the widened alveolar septum is infiltrated with more immune cells, including some cells which are CD200-positive (E, double-headed arrows). ATII expressing CD200 become more obvious in the pale background of injured tissues with reduced CD200 (E, arrows). Scale bars: 50 μm.

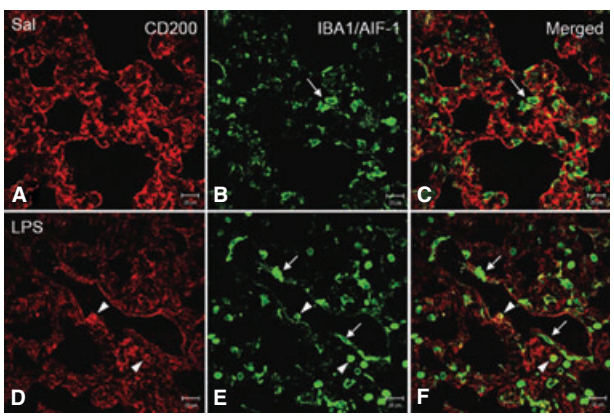

Fig. 6 (A–F) Expression of IBA1/AIF-1 and CD200 in lungs of rats treated with intratracheally instilled saline or LPS for 12 h. In the control or saline (A–C, Sal)-treated lungs, IBA1/AIF-1 marks immune cells including macrophages and T lymphocytes (B–C, arrows) in either the alveolar septum or the airspace. The labeled cells are irregular in outline. Following LPS challenge, CD200 immunoreactivity is reduced (D) and more IBA1/AIF-1-labeled cells are found, especially those which are long and irregular around the blood vessel (E–F, arrows), and round cells in the thickened septum and the lumen of blood vessel. Some IBA1/AIF-1-positive round cells unexpectedly express CD200 (E,F, arrowheads). Scale bars: 20 μm.

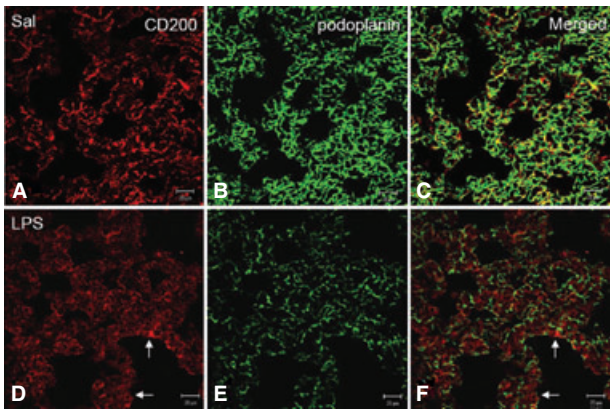

Fig. 7 (A–F) Expression of podoplanin and CD200 in lungs of rats intratracheally instilled with saline or LPS for 12 h. In the saline-treated (A–C, Sal) rats, patchy but intense CD200 immunoreactivity (A) is associated with podoplanin reaction products (B) in the control alveolar tissues. After LPS challenge, CD200 immunoreactivity diminishes and appears as diffused pattern with some positive cells in the thickened alveolar septum (D,F, arrows). Note that podoplanin immunoreactivity (B–C) is also noticeably reduced after LPS challenge (E,F). Scale bars: 20 μm.

thickened septum (Fig. 6A–F) where podoplanin immunoreactivity on type I pneumocytes also declined after LPS challenge (Fig. 7A–F).

Electron microscopic examination of LPS-challenged lung revealed that the intense immunoreactivity of CD200 on the thin portion of intact alveolar endothelia was either moderately decreased or completely abolished on the affected endothelia (Fig. 8A). The alveolar endothelia which exhibited normal CD200 expression showed vacuolations in the cytoplasm (Fig. 8B). Type II pneumocytes in the injured tissues showed similar changes in CD200 immunoreactivity, either a decrease or lack of it (Fig. 8C,D). Intravascular immune cells, such as granular leukocytes and monocytic cells, were mostly negative for CD200 (Fig. 8E); some lymphocytes contained CD200 (Fig. 8F). The immune cells were often closely associated with the alveolar endothelium (Fig. 8E,F).

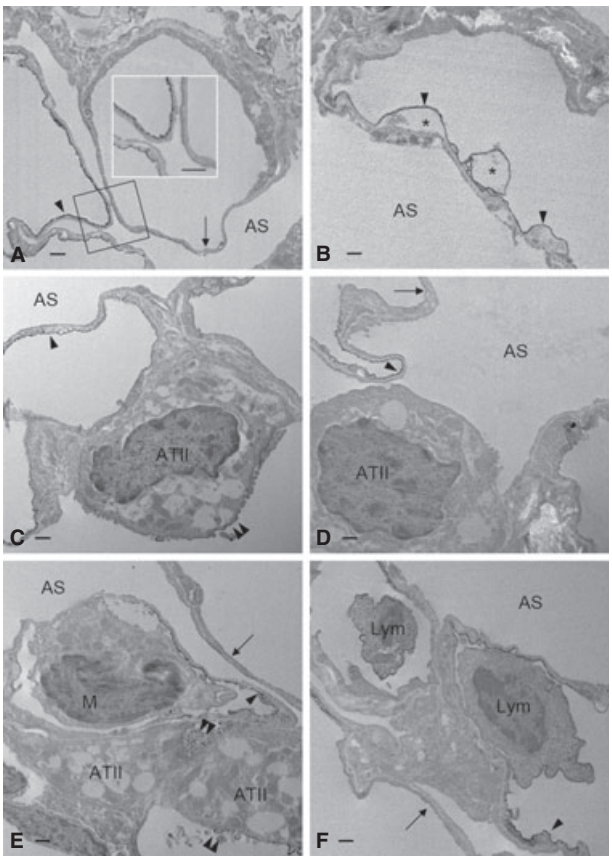

Fig. 8 (A–F) Electron micrographs showing CD200 expression in the distal airway of rat lungs challenged with LPS. CD200 is normally expressed on the luminal membrane of the alveolar endothelial cells, specifically on the thin portion that constitutes the blood–air barrier. A similar expression of CD200 is evidenced on the endothelia challenged with LPS (A–F, arrowheads). LPS markedly down-regulates CD200 expression on alveolar endothelia, which show lack of CD200 (A,D–F, arrows) or signs of degeneration with vacuolated cytoplasm (B, *). Endotoxin challenge does not affect CD200 expression (E, double arrowheads) significantly on alveolar type II epithelial cells (ATII); some of them display reduced amounts of CD200 (C, double arrowheads), whereas other display a total lack of CD200 (D). A monocytic cell (E,M), negative for CD200, is seen closely adherent to the thin portion of affected alveolar endothelium. The close cell contact is also evident between lymphocytes (F, Lym) and endothelial cells, both of which are CD200-positive. (Insert in A) Higher magnification of the structure outlined. AS, airspace. Scale bars: 500 nm.

Discussion

ATII are unique in the lung, synthesizing and secreting surfactant to maintain the integrity of the alveolar wall. Regarded as a target of the inflammatory response, ATII are involved in the modulation of development and resolution of the inflammatory reaction in the alveolar space (Hahon & Castranova, 1989; Janssen et al., 1998). Within the space, alveolar macrophages (AM) or pulmonary phagocytes located in close proximity to ATII and in contact with the surfactant lining are the first line of defense against inhaled microbes and particles (Lohmann-Matthes et al., 1994). The close association facilitates the intercellular communication between the two cell types. ATII are known to produce lung surfactant proteins such as surfactant-associated protein A and D (SP-A, SP-D), which are bound to the surfaces of host defense cells, promoting or inhibiting immune cell activity through multiple cellular pathways, in particular SP-D, which has a potent anti-inflammatory function (Kingma & Whitsett, 2006). In a co-culture system of human monocytes or THP-1 macrophages with monolayers of ATII-like cell line A549, Striz et al. (2001) had reported an epithelial cell induction of immune molecules (CD45 and HLA-DR) in cultured monocytes and macrophages. A dose-dependent increase in tumor necrosis factor alpha and MIP-2 release was also observed in the co-cultures with the AM and ATII

cell line, RLE-6TN (Tao & Kobzik, 2002). These studies suggest a significant role of ATII in regulating the phenotype and function of AM. In the present study, CD200 is expressed on Clara cells and cilia on some epithelial cells in the respiratory and terminal bronchioles; it is, however, absent on all epithelia in the trachea and bronchus. In the alveolar epithelium, type I pneumocytes were negative for CD200. On the other hand, ATII showed significant CD200 expression that was confined to microvilli-rich plasma membrane active in surfactant secretion. Very interestingly, CD200 was absent along the remaining plasma membrane facing the interstitium or type I pneumocytes. It is well documented that CD200 has an immunosuppressive function in immune reaction (Hoek et al., 2000; Dick et al., 2001; Broderick et al., 2002). Alveolar macrophages constitutively expressed CD200 receptors (Holt & Strickland, 2008; Snelgrove et al., 2008; Hussell & Cavanagh, 2009) and were closely associated with the epithelial surfaces in the terminal airspaces and tended to congregate at alveolar septal junctional zones (Parra et al., 1986; Holt et al., 1993). CD200 on the apical surface of ATII in the normal lung may initiate an inhibitory signal to AM adhesion through CD200R engagement to expel AM from the site where ATII are actively releasing their surfactants. The immunosuppressive effect of ATII CD200 on AM is in general agreement with the findings of Snelgrove et al. (2008). By flow cytometry and immunohistochemical staining, those authors concluded that all lung epithelial cells expressed CD200, which is the most likely means for controlling alveolar macrophages rich in CD200R expression. Our results, however, revealed only a limited expression of CD200 on the specific domain of ATII, Clara cells and some ciliated epithelial cells in the distal bronchioles of the normal rats. The expression patterns were hardly affected after LPS challenge. It is therefore suggested that the restricted and specific expression of CD200 on the lung epithelial cells may play a role in controlling the proper distribution of lung macrophages in normal condition; its involvement in immune homeostasis during heightened inflammation remains uncertain. Ciliated epithelium extending from the trachea to the terminal bronchioles is involved primarily in the mucociliary defense mechanism (Plotkowski et al., 1993). However, this specialized epithelium is diverse in its ciliary beat frequency (Clary-Meinesz et al., 1997) and tolerance to changes in external pH (Clary-Meinesz et al., 1998) dependent on localization. The heterogeneity of airway ciliated epithelium is further supported by our present results that showed CD200-expressing ciliated epithelia only in the bronchioles. The latter are sites vital to initial virus infection (Arndt et al., 2002) and lung inflammation (Betsuyaku et al., 2008). Among the epithelial cells in the bronchioles, Clara cells were well recognized to release important host defense molecules involved in regulating lung inflammation and immune activity (Wang et al., 2003; Reynolds et al., 2007). In contrast, the participation of bronchiolar ciliated epithelial cells (BCEC) in modulating the immune system has not yet been proven. The present study has shown a significant expression of CD200, an immune suppressor, on the ciliary membrane and axonemes of BCEC, suggesting a possible novel function of the cell in controlling hyperinflammatory responses of myeloid cell under normal and/or pathological conditions of the respiratory system.

The pulmonary tissues are absolutely modified to perform the transcapillary exchanges of gases. The exchange occurs at the site of the alveolar capillary unit constituting the so-called air–blood barrier, which is made up of the endothelial cells lining the capillaries and the epithelial cells that line the alveoli. A significant feature of the alveolar endothelium is the existence of two well-known domains within the same cell (Simionescu, 2001). An attenuated organelle-free area with few or no plasmalemmal vesicles is defined as an avesicular zone, where the endothelium is closely apposed with only alveolar type I epithelial cells. The other area containing numerous plasmalemmal vesicles is called the vesicular zone, in which the endothelium contacted with more interstitial cells or structures (Simionescu, 2001). It has been shown that the avesicular zone of the endothelial cell had very few or lacked anionic sites, whereas the plasma membrane in the vesicular area of endothelial cell bond cationized ferritin homogeneously (Simionescu & Simionescu, 1983). The micro-heterogeneity of alveolar endothelium has also been highlighted with two specific antibodies developed by Rorvik et al. (1988), who showed that over 95% of immunoreactivity was found on the thin portion of alveolar capillary wall. Moreover, the studies on a monoclonal antibody raised against an 85-kDa integral glycoprotein of endothelial plasma membrane demonstrated that this endothelial integral protein was closely associated with the attenuated, avesicular domain of the alveolar endothelium, but not with the other (vesicular) zone of the same endothelium (Ghitescu et al., 1999; Murciano et al., 2001). In the present study, we have also shown that lung CD200 was distributed preferentially on the pulmonary vein and microvascular endothelia. In the latter, CD200 was observed only on the luminal membrane along the thin portion of the alveolar endothelium but not on the thick portion of the same endothelium. On the basis of CD200 distribution, the present findings have provided further evidence supporting the concept of micro-heterogeneous domains in alveolar endothelium.

The respiratory tract comprises an easy and open entrance for microorganisms and other pathogenic particles in inhaled air. The first line of efficient defense is consequently required through the clearance by mucus flow, cilia propulsion and alveolar macrophages. Moreover, the rapid leukocyte extravasation from the lung vasculature seems to be an essential response of the host against the pathogens, and involves different CAMs, in particular those belonging to the immunoglobulin superfamily such as ICAM-1, VCAM-1 and platelet/endothelial cell adhesion molecule (PECAM).

So far, evidence showing the expression and function of CAMs in the pulmonary capillary endothelial cells is largely derived from studies on lung injuries and diseases. Data from the alveolar endothelial cells of normal animals are few and inconsistent. In healthy lungs of rodent and human, alveolar endothelial cells express constitutive ICAM-1 (Kang et al., 1993; Moreland et al., 2002; Basit et al., 2006; Perkowski et al., 2006) and PECAM (Vaporciyan et al., 1993; Bhatt et al., 2001; Perkowski et al., 2006). VCAM-1, either undetectable or inducible on alveolar capillaries, has been reported (Nakao et al., 1995; Feuerhake et al., 1998; Tamaru et al., 1998). The interaction of these endothelial CAMs with the corresponding ligands has been suggested to support the leukocyte adhesion to vascular endothelial cells and their transendothelial migration in the inflamed lungs (Vaporciyan et al., 1993; Moreland et al., 2002; Basit et al., 2006; Perkowski et al., 2006). Whether the CAMs are involved in the ordinary leukocyte migration into the alveolar space of the normal lungs remained unclear. As Burns et al. (2003) proposed, leukocytes emigrated preferentially at tricellular corners where the borders of three endothelial cells converged. Once having crossed the endothelium and its basement membrane through holes occupied by fibroblast contacts, leukocytes emerged into the interstitium, adhered to and spread on the surface of the fibroblast. The latter provided directional information and guided the leukocyte toward the alveolar subepithelial space through other holes in the basement membrane of type II pneumocyte. The leukocyte then migrated across the epithelium at another tricellular corner composed of the margins of two type I pneumocytes and a type II pneumocyte (Burns et al., 2003). This indicated a preferential route of leukocyte emigration to the airspace through the wide interstitium to avoid the interruption of gas exchange. Consequently, the concept that some inhibitory mechanisms exist to prevent leukocytes from migrating towards the alveolar space has been anticipated (Sibille & Reynolds, 1990). Our immunoelectron microscopic examination showed a unique distribution of CD200 immunoreactivity only on the luminal front of the attenuated side, also an active site of gas exchange, of alveolar endothelia. CD200, an adhesion molecule belonging to the IgG superfamily, has been known to acquire many immunosuppressive properties (Hoek et al., 2000; Dick et al., 2001; Broderick et al., 2002). It is therefore suggested that endothelial CD200 of alveolar capillary may exert an inhibitory effect of immune cell adhesion on the thin side of alveolar endothelia to keep the primary function in air exchange uninterrupted.

The modulation of CD200 expression in various cells and tissues under the stimulated or pathological condition has recently been elucidated. In the mode of psychophysical stress, exposure to inescapable shock could down-regulate the neuronal glycoprotein CD200 (Frank et al., 2007). CD200 protein and mRNA were significantly decreased in the hippocampus and inferior temporal gyrus of patients suffering from Alzheimer's disease (Walker et al., 2009). Koning et al. (2009) have also demonstrated a general decline of CD200 expression in multiple sclerosis lesions. These reports suggested that the decreased expression of neuronal CD200 may initiate a disturbed equilibrium in microglia–neuron interaction, in that way sensitizing the pro-inflammatory reactivity of microglia and resulting in CNS injures. In respiratory disorder, CD200 expression was drastically down-regulated during asthma exacerbation and that reduction was not related to infection (Aoki et al., 2009). Our present study showed a reduced expression of pulmonary CD200 beginning at 12 h; this decline was gradually stopped and expression restored at 24 h after LPS instillation into the rat trachea. Immunoelectron microscopic observation confirmed that alveolar endothelial CD200 was mainly responsible for the LPS-induced decline of lung CD200, indicating an early and acute response of endothelial CD200 in alveolar capillaries challenged with LPS. In our recent study on systemic and cultured endothelia, we have shown that LPS induced detectable changes of CD200 expression on the arteries normally expressing weak or no CD200, whereas changes on the accompanying veins and the capillaries rich in CD200 remained unaffected (Ko et al., 2009), indicating that endothelial CD200 expression could be differentially regulated by LPS. Additionally, we have shown that CD200 synthetic peptide could trigger CD200R signaling in macrophages to suppress their adhesion to the endothelium (Ko et al., 2009). In this connection, the early decrease in CD200 in the inflamed alveolar capillaries may represent a concurrent response with the increase of proinflammatory adhesion molecules after LPS challenge to assist the immune cell recruitment. The subsequent restoration of endothelial CD200 in the late inflammation may be a protective mechanism through the restraint of immune cell adhesion and prevent excess infiltration of immune cells. It is suggested that CD200 on alveolar endothelia may exert an immunosuppressive influence to control the normal infiltration of immune cells in the intact lung; furthermore, it is regulated by inflammatory factors to modulate immune cell recruitment and subsequent immune responses.

In parallel to our present results that showed a LPS-induced decline of CD200 in alveolar endothelia of rat lung, a recent study also reported a decrease of CD200 mRNA in the brain tissues at 1 year post LPS inoculation (Masocha, 2009). The mechanistic link between LPS challenge and down-regulation of CD200 remains unclear. Our immunoelectron microscopic examination revealed that degenerating alveolar endothelia still possessed significant CD200. It is therefore unlikely that the decline of endothelial CD200 resulted from cell death caused by LPS. It has been reported that the constitutive expression of CD200 is regulated by CCAAT/enhancer binding protein beta (C/EBP beta) (Chen et al., 2006). The C/EBP beta gene can encode several N-terminally truncated isoforms: liver-enriched activator protein (LAP) being a transcriptional activator in many

tissues and liver-enriched inhibitory protein (LIP) considered a functional antagonist of LAP. The LIP/LAP ratio is a critical factor in C/EBP beta-mediated gene transcription (Descombes & Schibler, 1991; Ossipow et al., 1993; Buck et al., 1994). During the LPS-mediated acute phase response, the steady-state level of C/EBP beta was noticeably augmented in many tissues including the lungs (Alam et al., 1992). In rat pulmonary microvascular endothelial cells, LAP and LIP isoforms could be induced by interleukin-1 beta and result in the induction of iNOS promoter that was strongly suppressed when LIP was over-expressed (Kolyada & Madias, 2001). In the light of the above, we speculate that LPS- regulated CD200 expression on lung alveolar endothelium may be a way of modulating the C/EBP beta isoform ratio.

Acknowledgements

This study was supported in part by research grants NSC94-2320-B-016-009 and NSC95-2320-B-016-003 (C. H. Wu) and NSC96-2320-B-006-037 (Y. F. Jiang-Shieh) from the National Science Council, Taiwan.

References

Alam T, An MR, Papaconstantinou J (1992) Differential expression of three C/EBP isoforms in multiple tissues during the acute phase response. *J Biol Chem* **267**, 5021–5024.

Aoki T, Matsumoto Y, Hirata K, et al. (2009) Expression profiling of genes related to asthma exacerbations. *Clin Exp Allergy* **39**, 213–221.

Arndt U, Wennemuth G, Barth P, et al. (2002) Release of macrophage migration inhibitory factor and CXCL8/interleukin-8 from lung epithelial cells rendered necrotic by influenza A virus infection. *J Virol* **76**, 9298–9306.

Barclay AN, Clark MJ, McCaughan GW (1986) Neuronal/lymphoid membrane glycoprotein MRC OX-2 is a member of the immunoglobulin superfamily with a light-chain-like structure. *Biochem Soc Symp* **51**, 149–157.

Bartling B, Hofmann HS, Weigle B, et al. (2005) Down-regulation of the receptor for advanced glycation end-products (RAGE) supports non-small cell lung carcinoma. *Carcinogenesis* **26**, 293–301.

Bartolome MV, Ibáñez-Olías MA, Gil-Loyzaga P (2002) Transitional expression of OX-2 and GAP-43 glycoproteins in developing rat cochlear nerve fibers. *Histol Histopathol* **17**, 83–95.

Basit A, Reutershan J, Morris MA, et al. (2006) ICAM-1 and LFA-1 play critical roles in LPS-induced neutrophil recruitment into the alveolar space. *Am J Physiol Lung Cell Mol Physiol* **291**, L200–207.

Beck-Schimmer B, Madjdpour C, Kneller S, et al. (2002) Role of alveolar epithelial ICAM-1 in lipopolysaccharide-induced lung inflammation. *Eur Respir J* **19**, 1142–1150.

Betsuyaku T, Hamamura I, Hata J, et al. (2008) Bronchiolar chemokine expression is different after single versus repeated cigarette smoke exposure. *Respir Res* **9**, 7–18.

Bhatt AJ, Pryhuber GS, Huyck H, et al. (2001) Disrupted pulmonary vasculature and decreased vascular endothelial growth factor, Flt-1, and TIE-2 in human infants dying with bronchopulmonary dysplasia. *Am J Respir Crit Care Med* **164**, 1971–1980.

Broderick C, Hoek RM, Forrester JV, et al. (2002) Constitutive retinal CD200 expression regulates resident microglia and activation state of inflammatory cells during experimental autoimmune uveoretinitis. *Am J Pathol* **161**, 1669–1677.

Buck M, Turler H, Chojkier M (1994) LAP (NF-IL-6), a tissue-specific transcriptional activator, is an inhibitor of hepatoma cell proliferation. *EMBO J* **13**, 851–860.

Burns AR, Smith CW, Walker DC (2003) Unique structural features that influence neutrophil emigration into the lung. *Physiol Rev* **83**, 309–336.

Chalepakis G, Wijnholds J, Giese P, et al. (1994) Characterization of Pax-6 and Hoxa-1 binding to the promoter region of the neural cell adhesion molecule L1. *DNA Cell Biol* **13**, 891–900.

Chen Z, Marsden PA, Gorczynski RM (2006) Cloning and characterization of the human CD200 promoter region. *Mol Immunol* **43**, 579–587.

Clark MJ, Gagnon J, Williams AF, et al. (1985) MRC OX-2 antigen: a lymphoid/neuronal membrane glycoprotein with a structure like a single immunoglobulin light chain. *EMBO J* **4**, 113–118.

Clary-Meinesz C, Mouroux J, Huitorel P, et al. (1997) Ciliary beat frequency in human bronchi and bronchioles. *Chest* **111**, 692–697.

Clary-Meinesz C, Mouroux J, Cosson J, et al. (1998) Influence of external pH on ciliary beat frequency in human bronchi and bronchioles. *Eur Respir J* **11**, 330–333.

Del Galdo F, Maul GG, Jiménez SA, et al. (2006) Expression of allograft inflammatory factor 1 in tissues from patients with systemic sclerosis and in vitro differential expression of its isoforms in response to transforming growth factor beta. *Arthritis Rheum* **54**, 2616–2625.

Descombes P, Schibler U (1991) A liver-enriched transcriptional activator protein, LAP, and a transcriptional inhibitory protein, LIP, are translated from the same mRNA. *Cell* **67**, 569–579.

Dick AD, Broderick C, Forrester JV, et al. (2001) Distribution of OX2 antigen and OX2 receptor within retina. *Invest Ophthalmol Vis Sci* **42**, 170–176.

Feuerhake F, Füchsl G, Welsch U (1998) Immunohistologic study of the localization of ICAM-1 (intercellular cell adhesion molecule 1) in alveolar epithelium in the human lung. *Pneumologie* **52**, 707–713.

Finzel AH, Reininger AJ, Bode PA, et al. (2004) ICAM-1 supports adhesion of human small-cell lung carcinoma to endothelial cells. *Clin Exp Metastasis* **21**, 185–189.

Frank MG, Barrientos RM, Biedenkapp JC, et al. (2006) mRNA up-regulation of MHC II and pivotal pro-inflammatory genes in normal brain aging. *Neurobiol Aging* **27**, 717–722.

Frank MG, Baratta MV, Sprunger DB, et al. (2007) Microglia serve as a neuroimmune substrate for stress-induced potentiation of CNS pro-inflammatory cytokine responses. *Brain Behav Immun* **21**, 47–59.

Ghitescu L, Jacobson BS, Crine P (1999) A novel, 85 kDa endothelial antigen differentiates plasma membrane macrodomains in lung alveolar capillaries. *Endothelium* **6**, 241–250.

Hahon N, Castranova V (1989) Interferon production in rat type II pneumocytes and alveolar macrophages. *Exp Lung Res* **15**, 429–445.

Hoek RM, Ruuls SR, Murphy CA, et al. (2000) Down-regulation of the macrophage lineage through interaction with OX2 (CD200). *Science* **290**, 1768–1771.

Holt PG, Strickland DH (2008) The CD200-CD200R axis in local control of lung inflammation. *Nat Immunol* **9**, 1011–1013.

Holt PG, Oliver J, Bilyk N, et al. (1993) Downregulation of the antigen presenting cell function(s) of pulmonary dendritic cells *in vivo* by resident alveolar macrophages. *J Exp Med* **177**, 397–407.

Hussell T, Cavanagh MM (2009) The innate immune rheostat: influence on lung inflammatory disease and secondary bacterial pneumonia. *Biochem Soc Trans* **37**, 811–813.

Janssen YM, Driscoll KE, Timblin CR, et al. (1998) Modulation of mitochondrial gene expression in pulmonary epithelial cells exposed to oxidants. *Environ Health Perspect* **106** (Suppl 5), 1191–1195.

Jaques G, Auerbach B, Pritsch M, et al. (1993) Evaluation of serum neural cell adhesion molecule as a new tumor marker in small cell lung cancer. *Cancer* **72**, 418–425.

Kang BH, Crapo JD, Wegner CD, et al. (1993) Intercellular adhesion molecule-1 expression on the alveolar epithelium and its modification by hyperoxia. *Am J Respir Cell Mol Biol* **9**, 350–355.

Kingma PS, Whitsett JA (2006) In defense of the lung: surfactant protein A and surfactant protein D. *Curr Opin Pharmacol* **6**, 277–283.

Ko YC, Chien HF, Jiang-Shieh YF, et al. (2009) Endothelial CD200 is heterogeneously distributed, regulated and involved in immune cell-endothelium interactions. *J Anat* **214**, 183–195.

Kolyada AY, Madias NE (2001) Transcriptional regulation of the human iNOS gene by IL-1beta in endothelial cells. *Mol Med* **7**, 329–343.

Koning N, Bö L, Hoek RM, et al. (2007) Downregulation of macrophage inhibitory molecules in multiple sclerosis lesions. *Ann Neurol* **62**, 504–514.

Koning N, Swaab DF, Hoek RM, et al. (2009) Distribution of the immune inhibitory molecules CD200 and CD200R in the normal central nervous system and multiple sclerosis lesions suggests neuron-glia and glia-glia interactions. *J Neuropathol Exp Neurol* **68**, 159–167.

Lohmann-Matthes ML, Steinmüller C, Franke-Ullmann G (1994) Pulmonary macrophages. *Eur Respir J* **7**, 1678–1689.

Masocha W (2009) Systemic lipopolysaccharide (LPS)-induced microglial activation results in different temporal reduction of CD200 and CD200 receptor gene expression in the brain. *J Neuroimmunol* **214**, 78–82.

McCaughan GW, Clark MJ, Barclay AN (1987) Characterization of the human homolog of the rat MRC OX-2 membrane glycoprotein. *Immunogenetics* **25**, 329–335.

Moreland JG, Fuhrman RM, Pruessner JA, et al. (2002) CD11b and intercellular adhesion molecule-1 are involved in pulmonary neutrophil recruitment in lipopolysaccharide-induced airway disease. *Am J Respir Cell Mol Biol* **27**, 474–480.

Murciano JC, Harshaw DW, Ghitescu L, et al. (2001) Vascular immunotargeting to endothelial surface in a specific macrodomain in alveolar capillaries. *Am J Respir Crit Care Med* **164**, 1295–1302.

Nakao A, Hasegawa Y, Tsuchiya Y, et al. (1995) Expression of cell adhesion molecules in the lungs of patients with idiopathic pulmonary fibrosis. *Chest* **108**, 233–239.

Ossipow V, Descombes P, Schibler U (1993) CCAAT/enhancer-binding protein mRNA is translated into multiple proteins with different transcription activation potentials. *Proc Natl Acad Sci U S A* **90**, 8219–8223.

Parra SC, Burnette R, Price HP, et al. (1986) Zonal distribution of alveolar macrophages, type II pneumonocytes, and alveolar septal connective tissue gaps in adult human lungs. *Am Rev Respir Dis* **133**, 908–912.

Perkowski S, Scherpereel A, Murciano JC, et al. (2006) Dissociation between alveolar transmigration of neutrophils and lung injury in hyperoxia. *Am J Physiol Lung Cell Mol Physiol* **291**, L1050–1058.

Petermann KB, Rozenberg GI, Zedek D, et al. (2007) CD200 is induced by ERK and is a potential therapeutic target in melanoma. *J Clin Invest* **117**, 3922–3929.

Plotkowski MC, Bajolet-Laudinat O, Puchelle E (1993) Cellular and molecular mechanisms of bacterial adhesion to respiratory mucosa. *Eur Respir J* **6**, 903–916.

Ragheb R, Abrahams S, Beecroft R, et al. (1999) Preparation and functional properties of monoclonal antibodies to human, mouse and rat OX-2. *Immunol Lett* **68**, 311–315.

Reynolds SD, Reynolds PR, Snyder JC, et al. (2007) CCSP regulates cross talk between secretory cells and both ciliated cells and macrophages of the conducting airway. *Am J Physiol Lung Cell Mol Physiol* **293**, L114–123.

Rorvik MC, Allison DP, Hotchkiss JA, et al. (1988) Antibodies to mouse lung capillary endothelium. *J Histochem Cytochem* **36**, 741–749.

Rosenblum MD, Olasz EB, Yancey KB, et al. (2004) Expression of CD200 on epithelial cells of the murine hair follicle: a role in tissue-specific immune tolerance? *J Invest Dermatol* **123**, 880–887.

Schulz C, Petrig V, Wolf K, et al. (2003) Upregulation of MCAM in primary bronchial epithelial cells from patients with COPD. *Eur Respir J* **22**, 450–456.

Sibille Y, Reynolds HY (1990) Macrophages and polymorphonuclear neutrophils in lung defense and injury. *Am Rev Respir Dis* **141**, 471–501.

Simionescu M (2001) Cellular components of the air-blood barrier. *J Cell Mol Med* **5**, 320–321.

Simionescu D, Simionescu M (1983) Differentiated distribution of the cell surface charge on the alveolar-capillary unit. Characteristic paucity of anionic sites on the air-blood barrier. *Microvasc Res* **25**, 85–100.

Snelgrove RJ, Goulding J, Didierlaurent AM, et al. (2008) A critical function for CD200 in lung immune homeostasis and the severity of influenza infection. *Nat Immunol* **9**, 1074–1083.

Striz I, Slavcev A, Kalanin J, et al. (2001) Cell-cell contacts with epithelial cells modulate the phenotype of human macrophages. *Inflammation* **25**, 241–246.

Tamaru M, Tomura K, Sakamoto S, et al. (1998) Interleukin-1beta induces tissue- and cell type-specific expression of adhesion molecules *in vivo*. *Arterioscler Thromb Vasc Biol* **18**, 1292–1303.

Tao F, Kobzik L (2002) Lung macrophage-epithelial cell interactions amplify particle-mediated cytokine release. *Am J Respir Cell Mol Biol* **26**, 499–505.

Vaporciyan AA, DeLisser HM, Yan HC, et al. (1993) Involvement of platelet-endothelial cell adhesion molecule-1 in neutrophil recruitment *in vivo*. *Science* **262**, 1580–1582.

Walker DG, Dalsing-Hernandez JE, Campbell NA, et al. (2009) Decreased expression of CD200 and CD200 receptor in Alzheimer's disease: a potential mechanism leading to chronic inflammation. *Exp Neurol* **215**, 5–19.

Wang SZ, Rosenberger CL, Bao YX, et al. (2003) Clara cell secretory protein modulates lung inflammatory and immune responses to respiratory syncytial virus infection. *J Immunol* **171**, 1051–1060.

Wright GJ, Puklavec MJ, Willis AC, et al. (2000) Lymphoid/neuronal cell surface OX2 glycoprotein recognizes a novel receptor on macrophages implicated in the control of their function. *Immunity* **13**, 233–242.